Effective dynamics for a spin-1/2 particle constrained to a space curve in an electric and magnetic field

Guo-Hua Liang,[1,*] Yong-Long Wang,[2] Meng-Yun Lai,[3] Hao Zhao,[1] Hong-Shi Zong,[1,4,5,†] and Hui Liu[1,‡]

[1]*National Laboratory of Solid State Microstructures, School of Physics, Collaborative Innovation Center of Advanced Microstructures, Nanjing University, Nanjing 210093, China*

[2]*School of Physics and Electronic Engineering, Linyi University, Linyi 276005, China*

[3]*College of Physics and Communication Electronics, Jiangxi Normal University, Nanchang 330022, China*

[4]*Department of Physics, Anhui Normal University, Wuhu, Anhui 241000, China*

[5]*Nanjing Proton Source Research and Design Center, Nanjing 210093, China*

(Received 10 February 2020; revised manuscript received 6 May 2020; accepted 11 May 2020; published 28 May 2020)

We consider the dynamics of a spin-1/2 particle constrained to move in an arbitrary space curve with an external electric and magnetic field applied. With the aid of gauge theory, we successfully decouple the tangential and normal dynamics and derive the effective Hamiltonian. A type of quantum potential called SU(2) Zeeman interaction appears, which is induced by the electric field and couples spin and intrinsic orbital angular momentum. Based on the Hamiltonian, we discuss the spin precession for the zero intrinsic orbital angular momentum case and the energy splitting caused by the SU(2) Zeeman interaction for a helix as examples, showing the combined effect of geometry and external field. The interaction may bring different approaches to manipulate quantum states in spintronics.

DOI: 10.1103/PhysRevA.101.053632

I. INTRODUCTION

The quantum dynamics in curved spacetime has interested scientists for a long time. Based on general relativity, the larger the curvature of spacetime, the stronger the gravitational field. In addition to astronomical surveys, it seems unlikely that we can investigate a large curvature effect in conventional laboratories. However, in recent decades, the technique for the synthesis of nanostructures has made great progress [1–4], which brings large space curvature to the laboratory.

These nanostructures with curved geometries provide a platform for studies of the dynamics in low-dimensional curved spaces, involving condensed matter [5–7], optics [8,9], and magnetism [10,11]. Because the curvature radius of the structures may reach the nanoscale, nontrivial curvature effects on quantum motion show up, which are not only important in theory but also indicate great application potential. For example, based on the effective continuum $\mathbf{k}\cdot\mathbf{p}$ model in curvilinear coordinates [6], it is proven that periodically bent quantum wires at the nanoscale with Rashba spin-orbit coupling generate topologically nontrivial insulating phases. In optics, inspired by the Schwarzschild metric, a paraboloid waveguide is constructed to show the curvature effect on the phase and group velocities of wave packets [9], which is consistent with the theoretical prediction from the effective paraxial equation in the curved space. It is also shown that curvature acts as an effective magnetic field in thin magnetic shells [10]. All of these phenomena indicate that when the curvature radius of the structure is closed to the characteristic length of the dynamics, geometric effects increase significantly, and methods in flat cases fail.

To effectively show the geometric effects by theory, one successful theoretical approach called the thin-layer procedure (TLP) or confining potential approach for investigation of the quantum mechanical properties of particles constrained to low-dimensional curved space was introduced [12,13]. TLP originally considers the limiting case of quantum mechanics in which a particle in three-dimensional (3D) Euclidean space is subject to a strong confining force acting in the normal direction of a curved surface and gives the effective two-dimensional (2D) Schrödinger equation. Interestingly, a geometric potential depending on the intrinsic and extrinsic curvature of the surface appears in this effective equation, showing the geometric effect in constrained systems. Later, this potential was demonstrated in photonic crystals [14]. Since TLP was introduced, many theoretical works have tried to develop and generalize this approach for the application in more situations, such as Schrödinger particle [15–17], charged particles in an electric and magnetic field [18–20], Dirac particles [21–23], spin-1/2 particles with the spin-orbital interaction [24–29], and an electromagnetic field [30–32] constrained to space curves and curved surfaces. More general cases of an arbitrary m-dimensional manifold embedded in an n-dimensional Euclidean space for spinless particles have also been carried out [33–37]. It is found that induced SO($n-m$) gauge fields are expected if the normal states are degenerate.

*guohua@nju.edu.cn
†zonghs@nju.edu.cn
‡liuhui@nju.edu.cn

Therefore, compared with the 2D case, 1D effective dynamics obtained by TLP from 3D Euclidean space shows a nontrivial SO(2) gauge potential as an augmented effect.

The geometrically induced gauge field for 1D optical or electronic wave guides is usually offered by the torsion when only the scalar property is considered, coupling to the intrinsic orbital angular momentum (IOAM) [38–40] or topological charge [41–43], while for the motion of spin-1/2 particles in curvilinear coordinates, spin connection acting as a non-Abelian gauge field appears, which is generated by local Lorentz transformation [44]. Besides the two geometrically induced gauge fields, a magnetic field and spin-orbit interaction due to an electric field can also be applied to 1D curved systems in terms of U(1) and non-Abelian gauge fields [45–49], respectively. Considering all these effects, the dynamics of a spin-1/2 particle constrained to a space curve in the presence of an electric and magnetic field seems intricate. It is our main aim here to give an effective Hamiltonian for a full description of this situation. Decoupling from the normal dynamics is the key step in TLP, which does not go well in some cases, especially when external fields are applied. In the past, the dynamics for a charged particle constrained to a space curve in an electric and magnetic field has been viewed as difficult to decouple.

However, it is found in Ref. [19] that by adopting an appropriate U(1) gauge, one can still get the effective 1D Hamiltonian successfully. In this paper, we go further to get the effective Hamiltonian for a spin-1/2 particle constrained to a space curve in the presence of an electric and magnetic field, by applying a suitable U(1) and SU(2) gauge. We show that the IOAM in a space wire couples to both the magnetic field and the SU(2) gauge field, which induces two types of Zeeman coupling.

The organization of the paper is as follows: In Sec. II, we derive the effective Hamiltonian for a spin-1/2 particle constrained to a space curve in an electric and magnetic field. In Sec. III, the spin orientation evolution is calculated for the ground state in normal directions based on the effective Hamiltonian. In Sec. IV, the energy band splitting and eigenstates in a helix are discussed. The final section contains a summary.

II. EFFECTIVE HAMILTONIAN FOR A SPIN-1/2 PARTICLE CONSTRAINED TO A CURVE

The appearance of the well-known geometric potential for scalar particles indicates that low-dimensional systems embedded in a 3D space show an extra geometric effect. As the internal degrees of freedom of the particle increase and external fields are applied, the extra geometric effects will be more and more complicated. Although spin-1/2 particles [21,24] and the effect of external electric and magnetic fields [19] have been studies for 1D constrained system separately, an analytical expression for the Hamiltonian including both of them has not been derived yet, and the corresponding geometric effects have not been fully displayed.

In this section, we follow the TLP to derive the effective Hamiltonian for a spin-1/2 particle confined to an arbitrary space curve $\mathcal{C}$, including the effect of an external magnetic and electric field. The effective Hamiltonian shall be valid for describing the dynamics of various 1D semiconducting nanostructures with an electric and magnetic field applied. To make it clear, the analytical derivations for the case without and with an electric and magnetic field are given in turn.

A. Without external fields

In 3D Euclidean space, the embedded curve $\mathcal{C}$ is parameterized by $\mathbf{r}(s)$ with s its arc length. We introduce orthogonal curvilinear coordinates (s, q_2, q_3) and Frenet frame; then, the neighborhood around the curve is described as

$$\boldsymbol{R}(s, q_2, q_3) = \mathbf{r}(s) + q_2\mathbf{n}(s) + q_3\mathbf{b}(s), \tag{1}$$

where $\mathbf{n}$ and $\mathbf{b}$ are the unit normal vector and binormal vector of $\mathcal{C}$, respectively. Applying the Frenet-Serret equations, we may write

$$\begin{pmatrix} \dot{\mathbf{t}} \\ \dot{\mathbf{n}} \\ \dot{\mathbf{b}} \end{pmatrix} = \begin{pmatrix} 0 & \kappa(s) & 0 \\ -\kappa(s) & 0 & \tau(s) \\ 0 & -\tau(s) & 0 \end{pmatrix} \begin{pmatrix} \mathbf{t} \\ \mathbf{n} \\ \mathbf{b} \end{pmatrix}, \tag{2}$$

where $\mathbf{t}$ is the unit tangent vector of $\mathbf{r}(s)$, the dot denotes the derivative with respect to the natural parameter s, and $\kappa(s)$ and $\tau(s)$ are the curvature and torsion of $\mathcal{C}$, respectively. In this frame, the metric tensor $G_{ij} = \partial_i\boldsymbol{R} \cdot \partial_j\boldsymbol{R}$, with $i, j = 1, 2, 3$, explicitly reads

$$G_{ij} = \begin{pmatrix} (1-\kappa q_2)^2 + \tau^2\left(q_2^2 + q_3^2\right) & -\tau q_3 & \tau q_2 \\ -\tau q_3 & 1 & 0 \\ \tau q_2 & 0 & 1 \end{pmatrix}. \tag{3}$$

At each point of the neighborhood, we can define the dreibeins e_i^I corresponding to the metric tensor $G_{ij} = e_i^I e_j^J \delta_{IJ}$, where δ_{IJ} is the flat metric and the capital letters I, J denote flat-space indices.

We choose I, J as the locally flat tangent space indices, then the dreibeins for the Frenet frame are written as

$$e_i^I = \begin{pmatrix} 1-\kappa q_2 & -q_3\tau & q_2\tau \\ 0 & 1 & 0 \\ 0 & 0 & 1 \end{pmatrix}. \tag{4}$$

Inversely, we have

$$e_I^i = \begin{pmatrix} \frac{1}{1-\kappa q_2} & \frac{q_3\tau}{1-\kappa q_2} & \frac{-q_2\tau}{1-\kappa q_2} \\ 0 & 1 & 0 \\ 0 & 0 & 1 \end{pmatrix}. \tag{5}$$

In 3D curvilinear coordinates, the nonrelativistic equation for a spin-1/2 particle in a confining potential $V_c(q_2, q_3)$ with the contribution of spin connection is

$$H = -\frac{1}{2m}\left[\frac{1}{\sqrt{G}}\nabla_i(\sqrt{G}G^{ij}\nabla_j)\right] + V_c(q_2, q_3), \tag{6}$$

where $\nabla_i = \partial_i + \Omega_i$, with the connection $\Omega_i = \frac{i}{4}\omega_{iIJ}\epsilon^{IJK}\sigma_K$, $G = \det(G_{ij})$. We work in units where $\hbar$ and light speed c are equal to unity throughout the paper. The spin connection is

$$\omega_{iIJ} = e_I^j\left(\partial_i e_{jJ} - \Gamma_{ij}^k e_{kJ}\right), \tag{7}$$

where Γ_{ij}^{k} are the usual Christoffel symbols. The wave function of the system $\Phi(s, q_2, q_3)$ should be normalized as

$$\int \sqrt{G}|\Phi|^2 ds dq^2 dq^3 = 1. \tag{8}$$

We assume that the confining potential $V_c(q_2, q_3)$ has a deep minimum on $\mathcal{C}$ in the Hamiltonian (6). We can use a harmonic oscillator potential to represent V_c approximately in the vicinity of $\mathcal{C}$, namely, $V_c(q_a) \approx \frac{m}{2}\omega^2 q_a^2$, with ω the proper frequency. To manipulate the potential, we introduce the dimensionless parameter ϵ and reexpress the confining potential as $V_c \approx \frac{m}{2\epsilon^2}\omega^2 q_a^2$. It is easy to find that the smaller ϵ, the deeper is the minimum of V_c, and the more the dynamics is squeezed on $\mathcal{C}$. Next, in the spirit of TLP, we do the rescaling [34] $q_a \to \sqrt{\epsilon} q_a$ $(a = 2, 3)$ and $H \to G^{1/4} H G^{-1/4}$, and introduce the new wave function $\Psi = G^{1/4}\Phi$. After the rescaling, V_c is a linear function of ϵ^{-1} approximately. Such a rescaling makes the parameter ϵ appear as a natural and dimensionless perturbative parameter in the theory. The parameter ϵ is assumed to be sufficiently small, so that most of the dynamics is squeezed on a quasi-1D system.

Before performing TLP, we have to give the explicit form of the spin connection. After some straightforward calculations, we find

$$\Omega_s = \frac{i}{2}(-\kappa\sigma_{\bar{3}} - \tau\sigma_{\bar{s}}) + O(\epsilon^{1/2}), \quad \Omega_2 = \Omega_3 = 0. \tag{9}$$

To be clear, the subscripts with a bar stand for the local flat indices I, J. It turns out that only the tangential component of the connection is nonzero, which makes the TLP easy to perform in this case.

Substituting the metric (3) and Eqs. (9) into the Hamiltonian (6) and expanding the rescaled Hamiltonian in the order of ϵ, we obtain

$$H = \frac{1}{\epsilon}H^{(-1)} + H^{(0)} + O(\epsilon^{1/2}), \tag{10}$$

where

$$H^{(-1)} = -\frac{1}{2m}\left(\partial_2^2 + \partial_3^2\right) + \epsilon V_c(q_2, q_3) \tag{11}$$

and

$$H^{(0)} = -\frac{1}{2m}(\partial_s + \Omega_s - i\tau\hat{L})^2 + V_g, \tag{12}$$

wherein the angular momentum operator is defined as $\hat{L} = -i(q_2\partial_3 - q_3\partial_2)$, and the geometric potential $V_g = -\frac{\kappa^2}{8m}$. $H^{(-1)}/\epsilon$ is the 2D Hamiltonian for a particle confined by the potential V_c, while Eq. (12) describes the dynamics of a spin-1/2 particle bounded to the curve.

Equation (12) is still not the effective 1D Hamiltonian required since the operator $\hat{L}$ is composed of normal derivatives. To get the availably effective Hamiltonian, we have to consider the eigenstates of the normal Hamiltonian (11). Because V_c is independent of s, we separate the rescaled wave function into tangential and normal wave functions, that is,

$$\Psi = \sum_{\beta} \psi_\beta(s)\chi_\beta(q_2, q_3), \tag{13}$$

where the index β labels the degeneracy in the spectrum of the normal Hamiltonian $H^{(-1)}$. The wave function $\chi(q_2, q_3)$ is totally determined by the confinement V_c. Here we only consider the case of a circular cross section, that is, V_c with SO(2) symmetry. More general case of the cross section has been discussed in Ref. [15] for the Schrödinger equation. In this case, it is convenient to make a coordinate transformation in the normal plane $(q_2, q_3) \to (r, \varphi)$, where $r = \sqrt{(q_2)^2 + (q_3)^2}$, $\varphi = \arctan(q_2/q_3)$. Then the normal eigenstates can be written as $\chi(r, \varphi)_{nl} = \frac{1}{\sqrt{2\pi}}R_n(r)e^{il\varphi}$, where $R_n(r)$ are normalized radial wave functions, and n and l are radial and angular quantum numbers, respectively. In the Hilbert space spanned by these normal eigenstates, the Hamiltonian (12) becomes a matrix with the elements

$$H^{(0)}_{nln'l'} = \int dr d\varphi r \chi_{nl} H^{(0)} \chi_{n'l'}. \tag{14}$$

It is easy to find that this matrix is diagonal, so we can write the effective Hamiltonian as

$$H_{\text{eff}} = -\frac{1}{2m}\left[(\partial_s + \Omega_s + i\tau l)^2 + \frac{\kappa^2}{4}\right]. \tag{15}$$

From Eq. (15), we find that for a spin-1/2 particle constrained to a space curve with a circular cross section, two geometrically induced gauge fields appear in the effective Hamiltonian, which can be separated into the spin angular momentum (SAM) part and the IOAM part. The SAM part depends on both the curvature and torsion of the space curve, while the IOAM part depends only on the torsion.

B. With an electric and magnetic field

In this section, we consider the case with an external electric field $\boldsymbol{E}$ and magnetic field $\boldsymbol{B}$ applied. The wave functions of nonrelativistic spin-1/2 particles in an external electromagnetic field satisfy the Pauli equation. It has been found [49] that the reformulation of the Pauli equation exhibits a basic U(1)× SU(2) gauge symmetry. This symmetry can be viewed as a fundamental property of nonrelativistic quantum mechanics. In the reformulated theory, the U(1) gauge field accounts for the interaction between the electromagnetic field and electric charge, and the SU(2) gauge field accounts for the Zeeman effect and spin-orbit coupling which determine the dynamics of the spin. It should be noted that the SU(2) gauge fields do not contain new physical variables, but functions of $\boldsymbol{E}$ and $\boldsymbol{B}$, which means the underlying interaction is still electromagnetic. The Lie algebra corresponding to the SU(2) group has standard mathematical representation, which consists of the traceless and Hermitian 2×2 complex matrices. Based on group theory, there are $2^2 - 1 = 3$ generators for the SU(2) group. The generators can be chosen as σ_x, σ_y, and σ_z, with $\boldsymbol{\sigma}$ the well-known Pauli matrices. Therefore, the SU(2) gauge field is also the function of Pauli matrices.

The nonrelativistic Hamiltonian for a spin-1/2 particle in an electric and magnetic field is of the form [47,49,50]

$$H = -\frac{1}{2m}\frac{1}{\sqrt{G}}D_i(\sqrt{G}G^{ij}D_j) - \mu_B \mathbf{B}\cdot\boldsymbol{\sigma} + eV, \tag{16}$$

where e is the electric charge, μ_B is the Bohr magneton, the covariant derivative $D_i = \nabla_i - ieA_i + i\frac{e}{4m}\epsilon_{ijk}\sigma^j E^k$, wherein A_i is the magnetic vector potential, and the last gauge term accounts for the spin-orbit interaction from the electric field.

The second term in Eq. (16) is the usual Zeeman coupling, and V is the scalar potential. Here we neglect the Darwin term and higher-order corrections. Formally, the gauge field can be divided into two parts: one is the U(1) gauge field A_i, the other is the SU(2) gauge field $\Omega_i + i\frac{e}{4m}\epsilon_{ijk}\sigma^j E^k$, with Ω_i the spin connection from the derivative ∇_i in Eq. (6). We denote that $W_i = i\Omega_i - \frac{e}{4m}\epsilon_{ijk}\sigma^j E^k$. In Yang-Mills gauge field theory, the covariant derivative is written as $D_\mu = \partial_\mu - igA^i_\mu\frac{\sigma^i}{2}$, with g the coupling constant. Following Yang-Mills theory, we can write the tangential and normal components of the gauge field as $W_s = i\Omega_s - \lambda w_{sj}\frac{\sigma^j}{2}$ and $W_a = -\lambda w_{aj}\frac{\sigma^j}{2}$, where $\lambda = -\frac{e}{2m}$ and $w_{ij} = \epsilon_{ijk}E^k$.

Before performing the confining potential approach, we have to note the gauge freedom of the electromagnetic vector potentials. Thus we need to expand the electromagnetic field potential in the vicinity of the space curve, that is,

$$A_i(s, \sqrt{\epsilon}q_a) = A_i(s, 0) + \sqrt{\epsilon}q_a\partial_a A_i(s, q_b)|_{q_b=0} + O(\epsilon). \tag{17}$$

Similarly, for the SU(2) gauge field, we can also expand it as

$$W_i(s, \sqrt{\epsilon}q_a) = W_i(s, 0) + \sqrt{\epsilon}q_a\partial_a W_i(s, q_b)_{q_b=0} + O(\epsilon). \tag{18}$$

Again, we introduce the confining potential V_c and expand the rescaled Hamiltonian up to zeroth order of ϵ and obtain

$$H = \frac{1}{\epsilon}H^{(-1)} + \frac{1}{\sqrt{\epsilon}}H^{(-1/2)} + H^{(0)} + O(\epsilon^{1/2}), \tag{19}$$

where

$$H^{(-1)} = -\frac{1}{2m}\left(\partial_2^2 + \partial_3^2\right) + \epsilon V_c(q_2, q_3), \tag{20}$$

$$H^{(-1/2)} = \frac{i}{m}(eA_a + W_a)\partial_a, \tag{21}$$

and

$$\begin{aligned} H^{(0)} = &-\frac{1}{2m}\left[(D_s + i\tau\hat{L})^2 + \frac{\kappa^2}{4}\right] + eV \\ &-\frac{1}{2m}[(-ieA_a - iW_a)^2 + \partial_a(-ieA_a - iW_a)] \\ &+\frac{i}{m}q_b\partial_b(eA_a + W_a)\partial_a - \mu_B\mathbf{B}\cdot\boldsymbol{\sigma}. \end{aligned} \tag{22}$$

Compared with the case without an external field, we find that a term of the order of $\epsilon^{-1/2}$ appears in the expression due to the external field applied. It seems from Eq. (21) that this term and the terms containing derivatives with respect to normal coordinates in Eq. (22) prevent the separation between the tangent and normal dynamics. In the following, we seek the appropriate gauge for the successful separation of the dynamics.

For the U(1) gauge field, we can find a gauge transformation $A_i' = A_i + \partial_i\gamma$, $\psi' = \psi e^{ie\gamma}$, where

$$\gamma = -A_a\sqrt{\epsilon}q^a + \frac{1}{2}\epsilon q^a q^b\partial_a A_b. \tag{23}$$

Then, after the gauge transformation, the electromagnetic field becomes

$$A_s' = A_s + O(\epsilon^{1/2}), \tag{24}$$

$$A_a' = -\sqrt{\epsilon}\frac{q^b}{2}F_{ab} + O(\epsilon), \tag{25}$$

where $F_{ab} = \partial_a A_b - \partial_b A_a$ is the electromagnetic field tensor.

Next we focus on the SU(2) gauge field W_a. Corresponding to the infinitesimal form of the fermion transformation $\psi \to (1 + \alpha_i\frac{\sigma^i}{2})\psi$, the transformation of the gauge field should be $w_{ai}\frac{\sigma^i}{2} \to w_{ai}\frac{\sigma^i}{2} + \frac{1}{\lambda}(\partial_a\alpha_i\frac{\sigma^i}{2}) + i[\alpha_i\frac{\sigma^i}{2}, w_{aj}\frac{\sigma^j}{2}]$. Now we define the SU(2) gauge transformation

$$\alpha_i\frac{\sigma^i}{2} = -\lambda\sqrt{\epsilon}q^a w_{ai}\frac{\sigma^i}{2} + \frac{\lambda}{2}\epsilon q^a q^b\partial_a\left(w_{bi}\frac{\sigma^i}{2}\right). \tag{26}$$

Applying this gauge transformation, we find the gauge field becomes

$$W_a' = -\frac{1}{2}\sqrt{\epsilon}q^b F_{abi}\frac{\sigma^i}{2}, \tag{27}$$

where we define the SU(2) field strength as

$$F_{abi}\frac{\sigma^i}{2} = \partial_a\left(w_{bi}\frac{\sigma^i}{2}\right) - \partial_b\left(w_{ai}\frac{\sigma^i}{2}\right) - 2i\lambda\left[w_{aj}\frac{\sigma^j}{2}, w_{bk}\frac{\sigma^k}{2}\right]. \tag{28}$$

As in the case of Eq. (24), for the tangential component W_s, we can also obtain $W_s' = W_s + O(\epsilon^{1/2})$ after the corresponding transformation. Hence, after the gauge transformations that we adopt, the tangential components of the gauge field remain unchanged.

Substituting Eq. (25) and Eq. (27) into the expansion (19), it is found the $\epsilon^{-1/2}$ order term vanishes and

$$\begin{aligned} H^{(0)} = &-\frac{1}{2m}\left[(D_s + i\tau\hat{L})^2 + \frac{\kappa^2}{4}\right] + eV \\ &+\lambda\left(F^{ab}L_{ab} + F_i^{ab}\frac{\sigma^i}{2}L_{ab}\right) - \mu_B\mathbf{B}\cdot\boldsymbol{\sigma}, \end{aligned} \tag{29}$$

where $L_{ab} = -i(q_a\partial_b - q_b\partial_a)$.

To obtain the effective Hamiltonian for the tangential dynamics, we still do the same procedure as the process from Eq. (13) to Eq. (15). Note that the field strength F^{ab} and $F_i^{ab}\frac{\sigma^i}{2}$ can be explicitly expressed into expressions of the external electric and magnetic field. The final form of the effective Hamiltonian for spin-1/2 particles constrained to a space curve in the presence of an electric and magnetic field is

$$H_{\text{eff}} = -\frac{1}{2m}\left[(D_s + i\tau l)^2 + \frac{\kappa^2}{4}\right] + eV + H_z, \tag{30}$$

where

$$H_z = -\mu_B\mathbf{B}\cdot\boldsymbol{\sigma} + 2\lambda B_s l + 2\lambda F_{so} l \tag{31}$$

and

$$F_{so} = (\nabla_\perp\cdot\boldsymbol{E}_\perp)\frac{\sigma_s}{2} - \left(\frac{\boldsymbol{\sigma}_\perp}{2}\cdot\nabla_\perp\right)E_s + \lambda(\boldsymbol{E}\cdot\boldsymbol{\sigma})E_s, \tag{32}$$

wherein $\perp$ stands for coordinates (q_2, q_3) in the normal plane of the curve, and $B_s = \boldsymbol{B}\cdot\boldsymbol{t}$ is the tangential component of the magnetic field. We can find that H_z contains three parts. The first one is the usual Zeeman coupling term composed of the magnetic field and spin angular momentum.

The second one is an induced Zeeman interaction between the tangential magnetic field and IOAM. The third one is a type of Zeeman interaction discovered in this paper, which is a coupling between IOAM and the SU(2) field strength, and we refer to it as the SU(2) Zeeman interaction. The necessary conditions of this interaction are $l \neq 0$ and the nonzero gradient of the electric field. Because of the Zeeman interaction, the spin and intrinsic orbital angular momentum no longer evolve independently. Equation (30) is the key result of the present paper, and the following discussions are based on this effective Hamiltonian.

III. SPIN PRECESSION FOR $l = 0$

In this section, we study the spatial behavior of spin precession for moving particles constrained to a space curve in the case of $l = 0$. To distinguish the effects of geometry and an external electric field, we still consider the case without and with an electric field in turn. No magnetic field is applied in this section.

A. Without external fields

Without external fields, the effective Hamiltonian (15) differs from the 1D free-electron Hamiltonian $H_f = -\frac{1}{2m}\partial_s^2$ only by a spin connection Ω_s as a gauge field and a geometric potential V_g. Therefore, by constructing a unitary transformation operator $U = e^{-\int \Omega_s ds}$, we obtain $U^\dagger H_{\text{eff}} U = H_f + V_g$. Correspondingly, if ψ is the eigenwave function of H_{eff}, $\psi_f = U^\dagger \psi$ is the eigenstate of $H_f + V_g$, retaining the spin state. This means the precession of the electrons can be described by the unitary transformation U. Considering the explicit form of Ω_s, we can always write the unitary transformation as

$$U = e^{\frac{i\boldsymbol{\sigma}\cdot\boldsymbol{h}\phi}{2}}, \tag{33}$$

where $\phi = \sqrt{\phi_c^2 + \phi_t^2}$ with $\phi_c = \int \kappa ds$ and $\phi_t = \int \tau ds$, and $\boldsymbol{h} = (-\tau/\phi, 0, -\kappa/\phi)^T$ is a unit vector in the Frenet coordinates. By using the formula

$$\exp\left(\frac{i\boldsymbol{\sigma}\cdot\boldsymbol{h}\phi}{2}\right) = \cos(\phi/2) + i\boldsymbol{\sigma}\cdot\boldsymbol{h}\sin(\phi/2), \tag{34}$$

we can directly calculate the spin orientation,

$$\langle\boldsymbol{\sigma}\rangle = \langle\psi_f|U^\dagger\boldsymbol{\sigma}U|\psi_f\rangle. \tag{35}$$

Further, the spatial derivatives of the expectation value of the spin components are obtained as

$$\partial_s\langle\boldsymbol{\sigma}\rangle = \langle[\Omega_s, \boldsymbol{\sigma}]\rangle + \langle\partial_s\boldsymbol{\sigma}\rangle. \tag{36}$$

We emphasize here that the spin connection is dreibein dependent. If one chooses the local flat tangent space coordinates, the spin connection is the form in Eq. (9), and $\partial_s\boldsymbol{\sigma} = (\partial_s e_I^i)\sigma^I = O(\epsilon^{1/2})$. Therefore, the commutator $\langle[\Omega_s, \boldsymbol{\sigma}]\rangle$ accounts for the precession. One can also choose the frame where the spin connection vanishes [51], and the final results are equivalent. Hence the spatial derivative of the spin orientation expectation has a matrix form,

$$\begin{pmatrix}\partial_s\langle\sigma_s\rangle\\ \partial_s\langle\sigma_2\rangle\\ \partial_s\langle\sigma_3\rangle\end{pmatrix} = \begin{pmatrix}0 & \kappa & 0\\ -\kappa & 0 & \tau\\ 0 & -\tau & 0\end{pmatrix}\begin{pmatrix}\langle\sigma_s\rangle\\ \langle\sigma_2\rangle\\ \langle\sigma_3\rangle\end{pmatrix}, \tag{37}$$

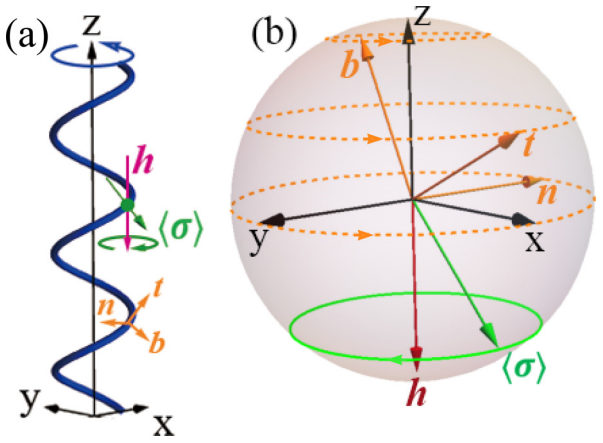

FIG. 1. (a) Schematic diagram of a helix. The parameter values are $r_0 = 1$, $d = 0.5$. Here the length unit is arbitrary. (b) Evolution of the spin orientation on the Bloch sphere for a spin-1/2 particle constrained to the helix.

or a compact form,

$$\partial_s\langle\boldsymbol{\sigma}\rangle = \phi\boldsymbol{h}\times\langle\boldsymbol{\sigma}\rangle. \tag{38}$$

From Eq. (38), we can see that $\boldsymbol{h}$ is, in fact, the instantaneous axis of rotation for spin orientation. Comparing Eq. (37) with Eq. (2), we find that they have a similar form. However, it should be note that in Eq. (2), the elements on the left side are derivatives of vectors, and in Eq. (37), they are derivatives of spin orientation expectation components. Therefore, the rotation of spin orientation may be different from the rotation of the vector in the Frenet frame.

To make it clear, we assume the space curve $\mathcal{C}$ is a helix [see Fig. 1(a)], which can be described in Cartesian coordinates as

$$x = r_0\cos\theta, \quad y = r_0\sin\theta, \quad z = d\theta. \tag{39}$$

It is easy to obtain the curvature $\kappa = \frac{r_0}{r_0^2+d^2}$, the torsion $\tau = \frac{d}{r_0^2+d^2}$, and the arc length $s = \sqrt{r_0^2+d^2}\theta$. We would like to exhibit the variation of the expectation value of the spin orientation in Cartesian coordinates, which would give an intuitional picture in a laboratory frame. In Cartesian coordinates, the spin gauge potential is simply written as $\Omega_s = -\frac{i}{2\sqrt{r_0^2+d^2}}\sigma_z$, since the axis of rotation $\boldsymbol{h}$ is found to be $-\boldsymbol{e}_z$. Then, we get the evolution of the spin orientation for a moving spin-1/2 particle constrained to a helix, which is shown in Fig. 1(b). It is found that moving along a helix leads to a spin orientation rotation in the opposite direction with respect to the rotation of the helix frame.

B. With a radial electric field

Now, for simplicity, we apply a uniform radial electric field $\boldsymbol{E}_r$ to the helix [see Fig. 2(a)]. In this case, $W_s = i\Omega_s + \frac{\lambda}{2}\sigma_3 E_0$, with E_0 the intensity of $\boldsymbol{E}_r$ at $r = r_0$. Since we assume the applied radial electric field is inward in the x-y plane and uniform along the z direction, E_0 is negative [see Fig. 2(b); the positive direction is outward]. The corresponding unitary transformation in this case should be $U' = e^{i\int W_s ds}$. We write

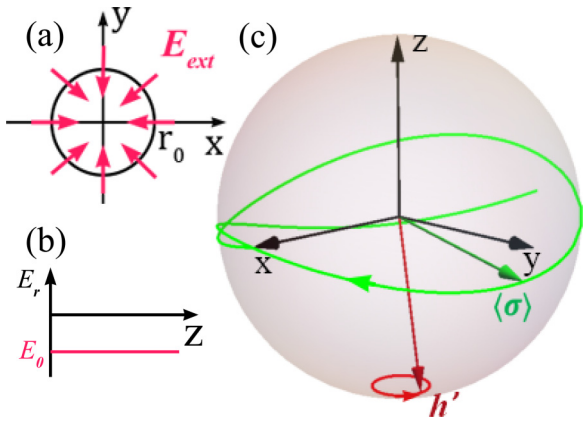

FIG. 2. (a) Schematic picture of the applied radial electric field in the x-y plane. The parameter values are $r_0 = l_E$, $d = 0.5l_E$ with the length unit $l_E = 1/2\lambda E_0$. (b) The independence of the electric field on z. (c) Evolution of spin orientation $\langle\boldsymbol{\sigma}\rangle$ and axis of rotation $\boldsymbol{h}'$ on the Bloch sphere in the laboratory frame.

the unitary transformation as $U' = e^{\frac{i\boldsymbol{\sigma}\cdot\boldsymbol{h}'\phi'}{2}}$, with

$$\boldsymbol{h}' = \left(\frac{-\tau}{\phi'}, 0, \frac{-\kappa - \lambda E_0}{\phi'}\right)^T, \tag{40}$$

and $\phi' = \sqrt{\phi_c'^2 + \phi_t^2}$, where $\phi_c' = \int \kappa + \lambda E_0 ds$. The vector $\boldsymbol{h}'$ is the instantaneous axis of rotation in the case that a radial electric field is applied. The variation of spin orientation in this case is shown in Fig. 2(c) for the length range $0 < \theta < 2\pi$, with the initial orientation along the x direction. One readily notes that the axis of rotation is no longer fixed, but rotates with the particle moving. Because of the rotation of axis $\boldsymbol{h}'$, the orientation of spin evolves to be more complex than the case without an external field. In addition, another difference caused by the external electric field is the extra rotation phase in ϕ_c'. This is why we find that the spin returns to its original orientation at a certain position θ_0 with $\theta_0 < 2\pi$, showing the property of Rashba spin-orbit interaction. The spin precession in this case indicates that the curvature is tantamount to provide an effective electric field.

The geometric effect in spin precession is closely related to the Berry's phase. In the case above, there is a twofold degeneracy in the system, which means the Berry phase factor should be generalized to an 2×2 matrix according to the theory of Wilczek and Zee [52]. We can write the matrix as $U(s) = \mathcal{P}\exp[i\int A_u(\boldsymbol{\lambda}(s))d\lambda^u]$, where $\mathcal{P}$ is the path-ordering operator, $\boldsymbol{\lambda}$ is the set of parameters, and $A_u = \langle\psi_\mu|i\partial_u|\psi_\nu\rangle$ (μ, ν are the degeneration indices and u is the parameter space index) is the connection acting as a non-Abelian gauge field. Based on the analysis above, if s is chosen as the parameter, the connection A_u is just the W_s. Alternatively, we can choose the spherical coordinates (ϑ, θ), which correspond to the sphere in Fig. 2, as the parameters. Then the Berry connections are $A_\vartheta = iU'^\dagger\partial_\vartheta U'$ and $A_\theta = iU'^\dagger\partial_\theta U'$. However, unlike the Abelian case, the phase change for the degenerated system cannot be shown by the solid angle subtended by the circuit in parameter space because no analog of Stokes' theorem exists for the non-Abelian case [53].

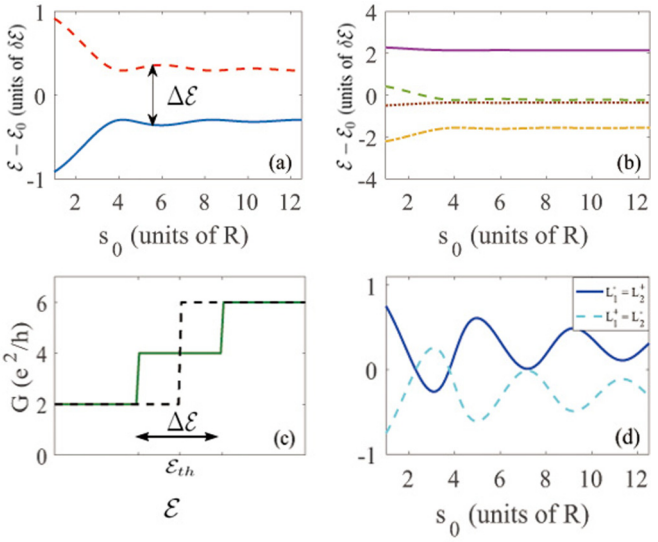

FIG. 3. Energy splitting in a helix as a function of total length for $l = \pm 1$ with (a) only the electric field and (b) both the electric and magnetic field ($\mu_B B_z = \delta\mathcal{E}$) applied. The unit $\delta\mathcal{E} = |\lambda(\partial_r E_r)|_{r=r_0}$ and $R = \sqrt{r_0^2 + d^2}$. The parameter values are $r_0 = l_E$, $d = 0.5l_E$. (c) Ballistic conductance at the vicinity of the threshold energy $\mathcal{E}_{th}$, in the case of $\partial_r E_r = 0$ (dashed line) and $\partial_r E_r \neq 0$ (solid line). (d) The expectation values of intrinsic orbital angular momentum $L_1^- = L_2^+$ (solid line) and $L_1^+ = L_2^-$ (dashed line) for the basis of the eigenvectors.

IV. ENERGY SPLITTING AND EIGENSTATES

In this section, we consider the effective dynamics in a helix for $l = \pm 1$ and mainly pay attention to the induced SU(2) Zeeman interaction. To ensure such a coupling term plays a role, we apply the helix of a radial electric field whose radial gradient is nonzero. In the following, we do a perturbation calculation on the energy levels in the helix for $l = \pm 1$.

The unperturbed Hamiltonian is $H_0 = -\frac{1}{2m}(D_s + i\tau l)^2 - \frac{\kappa^2}{8m} + eV$. We assume that the induced SU(2) Zeeman coupling and the magnetic field are sufficiently weak that they can be treated as a perturbation. In this case, according to Eq. (30), the perturbation is written as $H' = \lambda(\partial_r E_r)_{r=r_0}\sigma_s l + 2\lambda B_s l - \mu_B \boldsymbol{B}\cdot\boldsymbol{\sigma}$.

First, we assume $\boldsymbol{B} = 0$. Since κ and V are constant for the helix, it is easy to solve the eigenequation $H_0|s_t, l\rangle = \mathcal{E}_0|s_t, l\rangle$, and find the eigenvalue $\mathcal{E}_0 = \frac{1}{2m}(k^2 - \kappa^2/4) + eV$, and the degenerate eigenstates with the form $|s_t, l\rangle = e^{iks}e^{il\varphi}e^{i\int W_s ds}|s_t\rangle$, where $s_t = +, -$ with the definition $|+\rangle = (1, 0)^T$ and $|-\rangle = (0, 1)^T$. From degenerate perturbation theory, we obtain

$$\sum_{s_t', l'}[H'_{s_t' l', s_t l} - (\mathcal{E} - \mathcal{E}_0)\delta_{s_t' l', s_t l}]a_{s_t l} = 0, \tag{41}$$

with $\mathcal{E}$ the eigenvalue of $H_0 + H'$, and $a_{s_t l}$ the zeroth-order coefficients used to expand the perturbed states in terms of $|s_t, l\rangle$. Equation (41) yields eigenvalues $\mathcal{E}^\pm = \mathcal{E}_0 \pm \Delta\mathcal{E}/2$, which are shown in Fig. 3(a) as functions of the total length s_0. It is shown that the energy gap $\Delta\mathcal{E}$ varies with s_0 initially, and later tends to a definite value. The initial dependence

on the total length is caused by the spin precession that we present in the above section. This energy gap can be utilized to demonstrate the SU(2) Zeeman interaction experimentally. When the gradient of the electric field ($\partial_r E_r$) is zero, with the increasing of total energy, the conductance of the helical wire shows a steplike structure at the threshold energy $\mathcal{E}_{th}$ for $l = \pm 1$ [see the dashed line in Fig. 3(c)], while if we increase the value of $(\partial_r E_r)|_{r=r_0}$, a new plateau will appear in the conductance curve (the solid line) and the width of the plateau $\Delta\mathcal{E}$ will become wider since it is proportional to the gradient of the electric field. The energy splitting caused by the SU(2) Zeeman coupling reduces the degeneracy of the system from 4 to 2. The remaining degeneracy is due to the property of the SU(2) Zeeman interaction that its actions on $|s_t, l\rangle$ and $|-s_t, -l\rangle$ are the same. The associated eigenvectors are therefore still not determined completely because of the remaining degeneracy. However, we can write the bases of eigenvector for the energy $\mathcal{E}^+$ as

$$|\psi_1^+\rangle = a_o^+|+,-1\rangle + a_e^+|+,+1\rangle, \tag{42}$$

$$|\psi_2^+\rangle = a_o^+|-,+1\rangle + a_e^+|-,-1\rangle, \tag{43}$$

and the bases for the energy $\mathcal{E}^-$ as

$$|\psi_1^-\rangle = a_o^-|+,-1\rangle + a_e^-|+,+1\rangle, \tag{44}$$

$$|\psi_2^-\rangle = a_o^-|-,+1\rangle + a_e^-|-,-1\rangle, \tag{45}$$

where $a_o^\pm$ and $a_e^\pm$ can be determined from Eq. (41). To show the effect of the SU(2) Zeeman interaction on the states, we give the expectation of the intrinsic angular momentum for each eigenstate basis in Fig. 3(d), namely, $L_\mu^\pm = \langle\psi_\mu^\pm|\hat{L}|\psi_\mu^\pm\rangle$, with $\mu = 1, 2$ the degeneration index. It shows that $L_\mu^\pm$ oscillate with the total length and the amplitudes tend to reduce with s_0 increasing. Because of the degeneracy, we can find the relation $L_1^\pm = L_2^\mp$. When the total energy is in the range between $\mathcal{E}_{th} - \Delta\mathcal{E}/2$ and $\mathcal{E}_{th} + \Delta\mathcal{E}/2$, the channels $|\psi_1^-\rangle$ and $|\psi_2^-\rangle$ are open. In this case, if we drive purely spin-polarized particles into the system, the IOAM polarization may be expected.

The discussion above is for the case without an external magnetic field. Unlike the SU(2) Zeeman interaction induced by the radial electric field with nonzero gradient, Zeeman coupling for spin and IOAM due to a magnetic field could relieve the degenerate energy levels completely. In Fig. 3(b), we add the effect of a magnetic field B_z and plot the energy splitting against the total length. Comparing Figs. 3(a) and 3(b), it is obvious that the magnetic field relieves the partially degenerate energy levels in Fig. 3(a) and also breaks the symmetry of the energy levels about $\mathcal{E} = \mathcal{E}_0$.

V. CONCLUSION

To conclude, we have performed a thin-layer procedure to derive the effective Hamiltonian for a spin-1/2 particle constrained to a space curve in the presence of an electric and magnetic field. The difficulty on separation of the dynamics in the tangential and normal direction is overcome by a suitable choice of gauges. The final result shows that a quantum potential induced by the external electric field appears in the effective dynamics, which couples the spin and intrinsic orbital angular momentum, and can be described as the SU(2) Zeeman interaction. Based on the effective Hamiltonian, we have shown the spin precession in a helix without and with a radial electric field applied, in the case of zero intrinsic orbital angular momentum. It shows that the curvature can perform the role of an electric field, and the radial electric field rotates the instantaneous axis of rotation for the expectation of spin orientation. For the first-excited modes $l = \pm 1$, the energy splitting due to the SU(2) Zeeman interaction in a helix has been discussed. The SU(2) Zeeman interaction relieves the degeneracy partially and does not break the time-reversal symmetry, showing a different effect from the magnetic field.

Our derivation gives a full description of the nonrelativistic dynamics in a quasi-1D system including spin and an external electric and magnetic field. The theoretical results are applicable to various semiconducting nanowires when the electron rest mass and the Landé factor are replaced by their effective counterparts. The discovery of the SU(2) Zeeman interaction implies that in addition to the electric field intensity, the gradient of the electric field could be important for the manipulation of the nanowire system when the nonzero IOAM is considered. Experimentally, the dielectrophoresis [54], which is a powerful tool for generating high electric field gradients at nanoscale, may provide the environment required for the demonstration of this Zeeman interaction. Although we use the example of helical wires to show the energy splitting, a similar effect happens in quantum rings, which are easier to be realized experimentally. In the electric field, due to the Aharonov-Casher effect [55], the conductance of a quantum ring exhibits uniform oscillations as a function of the spin-orbit interaction strength. With the SU(2) Zeeman interaction added, the Berry phases of the system will be changed, which are associated with the energy band, spin, and intrinsic orbital angular momentum. Accordingly, the conductance signature will be changed. We expect the interaction to be demonstrated in such nanometer devices.

ACKNOWLEDGMENTS

This work is supported in part by the National Natural Science Foundation of China (Grants No. 11690030, No. 11475085, No. 11535005, and No. 61425018).

[1] S.-I. Park, A.-P. Le, J. Wu, Y. Huang, X. Li, and J. A. Rogers, Adv. Mater. **22**, 3062 (2010).

[2] L. A. B. Marcal, B. L. T. Rosa, G. A. M. Safar, R. O. Freitas, O. G. Schmidt, P. S. S. Guimaraes, C. Deneke, and A. Malachias, ACS Photon. **1**, 863 (2014).

[3] Z. Ren and P.-X. Gao, Nanoscale **6**, 9366 (2014).

[4] Q. Sun, R. Zhang, J. Qiu, R. Liu, and W. Xu, Adv. Mater. **30**, 1705630 (2017).

[5] C.-H. Chang, J. van den Brink, and C. Ortix, Phys. Rev. Lett. **113**, 227205 (2014).

[6] P. Gentile, M. Cuoco, and C. Ortix, Phys. Rev. Lett. **115**, 256801 (2015).
[7] J. S. Vorobyova, A. B. Vorob'ev, V. Y. Prinz, A. I. Toropov, and D. K. Maude, Nano Lett. **15**, 1673 (2015).
[8] R. Bekenstein, J. Nemirovsky, I. Kaminer, and M. Segev, Phys. Rev. X **4**, 011038 (2014).
[9] R. Bekenstein, Y. Kabessa, Y. Sharabi, O. Tal, N. Engheta, G. Eisenstein, A. J. Agranat, and M. Segev, Nat. Photon. **11**, 664 (2017).
[10] Y. Gaididei, V. P. Kravchuk, and D. D. Sheka, Phys. Rev. Lett. **112**, 257203 (2014).
[11] R. Streubel, P. Fischer, F. Kronast, V. P. Kravchuk, D. D. Sheka, Y. Gaididei, O. G. Schmidt, and D. Makarov, J. Phys. D **49**, 363001 (2016).
[12] H. Jensen and H. Koppe, Ann. Phys. **63**, 586 (1971).
[13] R. C. T. da Costa, Phys. Rev. A **23**, 1982 (1981).
[14] A. Szameit, F. Dreisow, M. Heinrich, R. Keil, S. Nolte, A. Tünnermann, and S. Longhi, Phys. Rev. Lett. **104**, 150403 (2010).
[15] S. Takagi and T. Tanzawa, Prog. Theor. Phys. **87**, 561 (1992).
[16] J. Stockhofe and P. Schmelcher, Phys. Rev. A **89**, 033630 (2014).
[17] Y.-L. Wang, M.-Y. Lai, F. Wang, H.-S. Zong, and Y.-F. Chen, Phys. Rev. A **97**, 042108 (2018).
[18] G. Ferrari and G. Cuoghi, Phys. Rev. Lett. **100**, 230403 (2008).
[19] F. T. Brandt and J. A. Sánchez-Monroy, Europhys. Lett. **111**, 67004 (2015).
[20] Y.-L. Wang and H.-S. Zong, Ann. Phys. **364**, 68 (2016).
[21] P. Ouyang, V. Mohta, and R. Jaffe, Ann. Phys. **275**, 297 (1999).
[22] M. Burgess and B. Jensen, Phys. Rev. A **48**, 1861 (1993).
[23] F. Brandt and J. Sánchez-Monroy, Phys. Lett. A **380**, 3036 (2016).
[24] C. Ortix, Phys. Rev. B **91**, 245412 (2015).
[25] M. V. Entin and L. I. Magarill, Phys. Rev. B **64**, 085330 (2001).
[26] J.-Y. Chang, J.-S. Wu, and C.-R. Chang, Phys. Rev. B **87**, 174413 (2013).
[27] Y.-L. Wang, L. Du, C.-T. Xu, X.-J. Liu, and H.-S. Zong, Phys. Rev. A **90**, 042117 (2014).
[28] Y.-L. Wang, H. Jiang, and H.-S. Zong, Phys. Rev. A **96**, 022116 (2017).
[29] G.-H. Liang, Y.-L. Wang, M.-Y. Lai, H. Liu, H.-S. Zong, and S.-N. Zhu, Phys. Rev. A **98**, 062112 (2018).
[30] S. Batz and U. Peschel, Phys. Rev. A **78**, 043821 (2008).
[31] M.-Y. Lai, Y.-L. Wang, G.-H. Liang, F. Wang, and H.-S. Zong, Phys. Rev. A **97**, 033843 (2018).
[32] M.-Y. Lai, Y.-L. Wang, G.-H. Liang, and H.-S. Zong, Phys. Rev. A **100**, 033825 (2019).
[33] P. Maraner and C. Destri, Mod. Phys. Lett. A **08**, 861 (1993).
[34] P. Maraner, J. Phys. A: Math. Gen. **28**, 2939 (1995).
[35] P. Maraner, Ann. Phys. **246**, 325 (1996).
[36] K. Fujii, N. Ogawa, S. Uchiyama, and N. M. Chepilko, Int. J. Mod. Phys. A **12**, 5235 (1997).
[37] P. Schuster and R. Jaffe, Ann. Phys. **307**, 132 (2003).
[38] A. T. O'Neil, I. MacVicar, L. Allen, and M. J. Padgett, Phys. Rev. Lett. **88**, 053601 (2002).
[39] K. Y. Bliokh, F. J. Rodríguez-Fortuño, F. Nori, and A. V. Zayats, Nat. Photon. **9**, 796 (2015).
[40] D. L. P. Vitullo, C. C. Leary, P. Gregg, R. A. Smith, D. V. Reddy, S. Ramachandran, and M. G. Raymer, Phys. Rev. Lett. **118**, 083601 (2017).
[41] M. S. Soskin, V. N. Gorshkov, M. V. Vasnetsov, J. T. Malos, and N. R. Heckenberg, Phys. Rev. A **56**, 4064 (1997).
[42] G. Molina-Terriza, J. Recolons, J. P. Torres, L. Torner, and E. M. Wright, Phys. Rev. Lett. **87**, 023902 (2001).
[43] L. Wang, M. Troyer, and X. Dai, Phys. Rev. Lett. **111**, 026802 (2013).
[44] G. t Hooft, *50 Years of Yang-Mills Theory* (World Scientific, Singapore, 2005).
[45] A. Rebei and O. Heinonen, Phys. Rev. B **73**, 153306 (2006).
[46] P.-Q. Jin, Y.-Q. Li, and F.-C. Zhang, J. Phys. A **39**, 7115 (2006).
[47] B. Leurs, Z. Nazario, D. Santiago, and J. Zaanen, Ann. Phys. **323**, 907 (2008).
[48] E. Medina, A. López, and B. Berche, Europhys. Lett. **83**, 47005 (2008).
[49] J. Fröhlich and U. M. Studer, Rev. Mod. Phys. **65**, 733 (1993).
[50] J. Fröhlich and U. Studer, Commun. Math. Phys. **148**, 553 (1992).
[51] Z.-J. Ying, P. Gentile, C. Ortix, and M. Cuoco, Phys. Rev. B **94**, 081406(R) (2016).
[52] F. Wilczek and A. Zee, Phys. Rev. Lett. **52**, 2111 (1984).
[53] J. W. Zwanziger, M. Koenig, and A. Pines, Annu. Rev. Phys. Chem. **41**, 601 (1990).
[54] A. Kuzyk, Electrophoresis **32**, 2307 (2011).
[55] Y. Aharonov and A. Casher, Phys. Rev. Lett. **53**, 319 (1984).